SSRG International Journal of Civil Engineering
ISSN: 2348-8352/ https://doi.org/10.14445/23488352/IJCE-V13I7P116

Volume 13 Issue 7, 254-261, July 2026
© 2026 Seventh Sense Research Group®

Original Article

Optimization of Solar Efficiency in Civil Infrastructure: Design and Structural Validation of an Automated Maintenance Device for Solar Panels

Albert Jorddy Valenzuela Inga[1*], Tania Mishel Vásquez Montoya[2], Nelfa Estrella Ayuque Almidon[1], Carlos Quispe Anccasi[3], Boris Senin Carhuallanqui Parian[4]

[1]*Escuela de Posgrado Continental, Universidad Continental, Lima, Peru.*
[2]*Facultad de Arquitectura, Universidad César Vallejo, Lima, Peru.*
[3]*School of Electrical Engineering, Universidad Continental, Lima, Peru.*
[4]*Institute for Statistical Studies and Economics of Knowledge (ISEEK), HSE University, Moscow, Russia.*

[*]*Corresponding Author : 73449915@continental.edu.pe*

Received: 31 March 2026 Revised: 01 June 2026 Accepted: 02 July 2026 Published: 29 July 2026

Abstract *- Photovoltaic devices are commonly used in civil engineering as they provide a sustainable energy source for infrastructure. However, dust accumulation on these devices can cause an efficiency loss between 15% and 40%. Current automated cleaning solutions often lack a detailed structural assessment an as consequence of the risk of mechanical failure in the long-term increases. In this study, a photovoltaic cleaning device -that can be integrated in a non-invasive way in existing photovoltaic supporting frames-and its preliminary structural assessment is presented. The structural assessment was divided into to operation modes called Service Case and Strength Design Case. The latter one applied a factored load. In the service case, the device evidences a maximum von Mises stress of 8.79 MPa and a displacement of 0.145 mm. In contrast, in the Strength Design Case, which uses factored loads, a stress of 14.298 MPa and a displacement of 0.235 was found; the safety factor for both cases was 15. These results indicate that designed single-axis devices evidenced a suitable preliminary structural response under static loading conditions. Compared to rotary or drone cleaning solutions, the presented design is less complex as it used linear guided motion. The cleaning efficiency, dynamic response, wind effects, or long-term durability were out of the scope of the study and would require prototyping. The presented devices provide a useful way of maintaining photovoltaic panels in existing structures and increase the adoption of this renewable energy in civil engineering, developing infrastructures.*

Keywords *- Automated maintenance, Civil infrastructure, Finite element method, Photovoltaic systems, Solar panel cleaning.*

1. Introduction

In order to promote global carbon neutrality, the integration of renewable energy systems in civil engineering infrastructure is necessary. [1, 2]. Photovoltaic (PV) systems have demonstrated scalability and affordable cost in residential, commercial and industrial developments [3, 4]. However, the viability of these applications depends on maintenance to sustain the operative efficiency during the entire life cycle of the infrastructure. Operative efficiency is essential to guarantee constant energy production both to attain sustainability objectives and complete the project return on investment in civil engineering [5, 6]. Previous studies have pointed out that dust, particles, bird droppings, and pollutant accumulation are the main causes of the decrease in PV efficiency [7, 8]. Najmi et al. [9] highlighted that dust acts essentially as a physical barrier that blocks sunlight-which can cause a power reduction of 86% in severe cases-and that regular cleaning is necessary to maintain operative efficiency. Dust accumulation in arid regions can cause a power reduction in the range of 15-35%, and its variation depends on the exposure time [10, 11]. Manual cleaning of PV systems requires safe access to the panel surface, maintenance planning, and water availability [9, 12]. Consequently, automated alternatives such as drone-based cleaning provide a non-contact method they use the thrust generated by the drone itself to remove the dust from the PV surface [13]. Similarly, other water-free approaches are based on air flow, brushes, or rotary elements [14]; these solutions are especially useful in dry regions. Although the aforementioned solutions are automated, they come with moving parts that can cause vibration and are often mechanically complex.

The design of robotic and automate cleaning solutions requires structural analysis in order to avoid excessive loads, stress concentration, and displacement on the PV module or its support frame. Shen et al. [15] presented a cleaning robot

This is an open access article under the CC BY-NC-ND license (http://creativecommons.org/licenses/by-nc-nd/4.0/)

based on a monorail bogie for solar panels in which the end-effector position and orientation were relevant to the cleaning process. Murshiduzzaman et al. [16] highlighted the relevance of the structural design of cleaning robots and their impact on efficiency and long-term damage from the PV-cleaning robot interaction. Another study presented linear-drive cleaning systems as an alternative to rotary and transmission mechanisms; the use of guided linear motion is presented as a suitable solution for photovoltaic cleaning applications [17]. From the aforementioned studies, it can be seen that structural assessment is a preliminary step prior to manufacturing the automated cleaning device. Automated and guided PV cleaning devices have also reached into patents field; these devices include wiper blades, nozzles, actuators, guide rails, mobile frames, rotary brushes, and elements that supply water [18, 19]. Similarly, in these patents, a detailed structural assessment that considers the applied loads under the operative service of these devices is lacking. Based on the conducted review, a simplified cleaning device for PV panels that can be integrated into the PV structure and that considers the structural assessment of the whole system is required.

In this study, we conduct a structural assessment of a proposed design of an automated cleaning device with a single-axis linear motion. The device consists of two lateral rails, one located at each lateral side of the solar panel. Furthermore, we included a mobile carriage driven by belts and a square tube where a rubber wiper is supported, similar to the cleaning blades that are used in vehicle windshields, in which water is supplied to assist the cleaning process. The novelty of the design is that-in contrast to robotic systems or a rotary brush-it reduces the mechanical complexity through the lateral supports, reducing the applied load on the PV and redirecting it to the rails and supporting structure. In addition, the structural assessment is carried out through Finite Element Analysis (FEA) in Autodesk Inventor; this structural verification represents a valuable prior step to prototyping or field testing as it identifies stress concentration zones, displacements, and safety factors. In summary, the proposed PV cleaning device design is novel, and the present approach provides a basis for future prototyping or a basis for improving into a new generation of cleaning devices.

2. Methodology

2.1. Geometric Modeling

The present analysis is limited to a static structural response (in Autodesk Inventor) of critical parts of the cleaning device using FEA analysis. Therefore, fatigue, dynamic effects or power consumption are out of the scope of the present study. An isometric view of the PV cleaning device, including its dimensions, is shown in Figure 1. To provide a better insight into the proposed design, an exploded view of the assembly and highlighting its main components, Figure 2 displays the components in a systematic way. The assembly consists of seven main components: a cleaning arm, wheel plates, support brackets, a rubber wiper, the water supply tuber, PV, the guiding rails and the supporting structure. The list of components is depicted in Table 1, including material specifications.

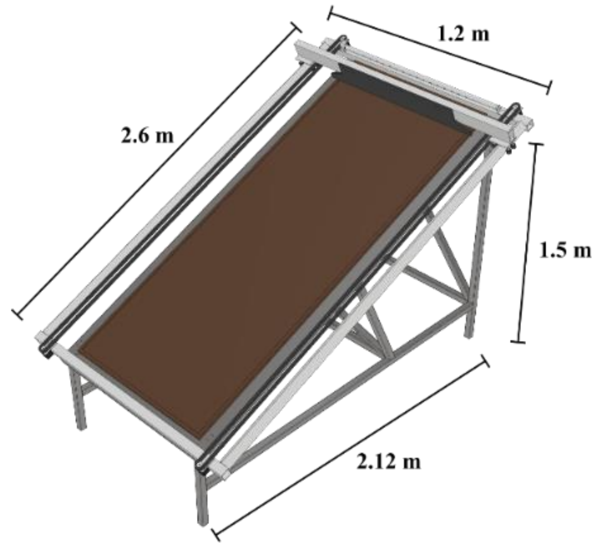

Fig. 1 General isometric view of the proposed water-assisted photovoltaic panel cleaning device

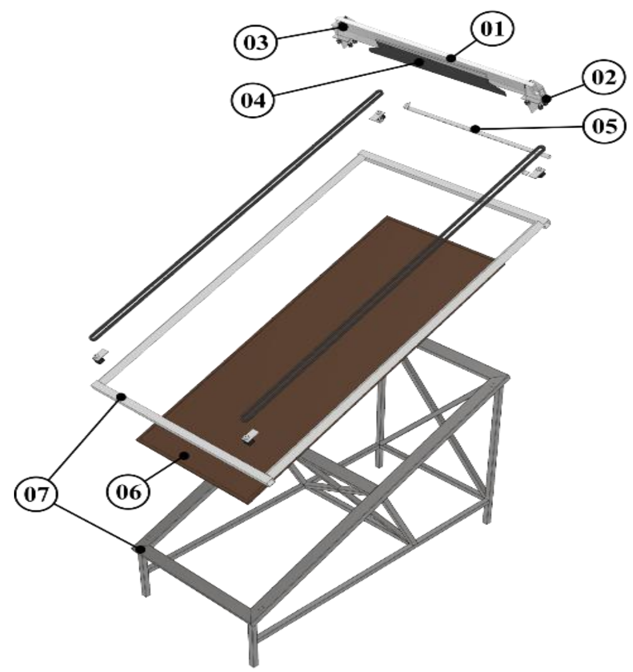

Fig. 2 Exploded view of the proposed cleaning device showing the main mechanical components and assembly sequence

Table 1. List of components

Nº	Component	Material Specification
01	Cleaning arm	Aluminum 6061-T6 82,55 x 25,4 x 1.5 mm
02	Wheel plates / mobile carriage	Aluminum 6061-T6

	plates	
03	Angular support brackets	ABS plastic
04	Rubber wiper	EPDM rubber, excluded from structural FEA
05	Water supply tube	Included in conceptual design, excluded from structural FEA
06	Solar panel	Tempered glass
07	Rails and base support	Fixed boundary conditions in the simplified FEA model

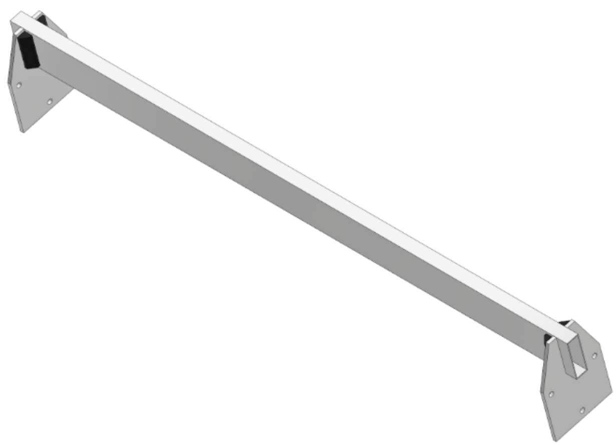

Fig. 3 Simplified structural model of the cleaning arm and support components used for the finite element analysis.

The FEA analysis is carried out in the components that are subjected to loads, this includes the cleaning arm, the wheel plates, and the support brackets. Figure 3 shows the geometry used for the FEA analysis. It must be mentioned that threads, screws, electrical wiring, or the rubber wiper are not included in the simplified geometry, as the focus is solely on the static structural response under normal operation conditions. In addition to that, the reduced geometry also reduces the meshing generation complexity.

2.2. Material Selection

In order to select a material for each component, the main factor for the decision is the applied loads into the simplified structural model depicted in Figure 3. In this regard, the horizontal cleaning arm and the wheel plates are defined as made of an Aluminum 6061-T6. This type of aluminum is characterized by its high strength-to-weight ratio; for this reason, this material is commonly used in lightweight structures [20]. In the Autodesk Inventor material selection, the database for this type of aluminum includes the following properties: Young's module of 72.7 GPa, a Poisson's ratio of 0.33, yield strength of 313 MPa, and an ultimate tensile strength of 340 MPa. The angular support brackets-which are similar to commercially available angular support for light assemblies-are assigned as an ABS plastic.

The ABS plastic presents the following properties: density of 1.06 g/cm³, Young's modulus of 2.24 GPa, Poisson's ratio of 0.38, yield strength of 20 MPa, and an ultimate tensile strength of 29.6 MPa. As mentioned earlier, although the cleaning device requires screws, these are not considered in the FEA analysis; instead, the connections are represented as bounded contacts. However, the effect of the rubber wiper and the perforated water supply tube are represented through applied normal pressure and a tangential frictional force on the cleaning arm.

2.3. Finite Element Model Setup

In Autodesk Investor, the structural simulation is carried out considering a linear static analysis. Autodesk allows an automatic mesh generation by setting up a few parameters, such as average element size (defined as 0.1), minimum element size (set as 0.2 of the average size), grading factor (defined as 1.5), and the maximum turn angle (60°). In addition to that, curved mesh elements are deactivated.

The contact type between the cleaning arm, ABS support brackets, and the wheel plates are set as bonded contacts; this approach simplifies the screw and fastened connections under a static load. In this sense, instead of focusing on the stress of each fastener (screws, holes, washers, or local threads), the focus is on the static response of the main structure assembly. In addition, a fixed constraint is applied in the interface between the assembly and the supporting structure. The resulting finite element data includes von mises stress, total displacements, contact pressures, reaction forces, and safety factors. Subsequently, the obtained values are interpreted based on the defined material for each component.

2.4. Boundary Conditions and Loads

Two static load scenarios are defined for the structural assessment of the PV cleaning devices. The first scenario is called the Service Case (SC); this scenario represents the normal cleaning conditions of the device.

The second scenario, which represents a high demand or load condition, is called the Strength Design Case (SDC). The latter case allows us to verify the structural integrity under an increased applied load. In this sense, the two-case approach allows us to evaluate the PV cleaning devices under to regimens and goes beyond the normal loading conditions. This criterion is consistent with the structural assessment of PV panels carried out by Murshiduzzaman et al. [16] and with the factored load principles that are widely employed in structural design [21].

2.4.1. Gravitational Load

In the Service Case, standard gravity was g = 9,81 m/s², equivalent to 9810 mm/s², to represent the self-weight of the assembly. In the Strength Design Case, gravity was increased to 11770 mm/s², corresponding approximately to 1.2 times the standard gravitational load.

2.4.2. Cleaning Pressure

Under normal cleaning conditions, a normal pressure acts in the lower region of the cleaning arm. Although the rubber wiper is not included in the geometrical modeling, its effect is represented as an equivalent pressure.

Consequently, the pressure of 15 N/m is assumed along a cleaning length of 1.2 m; these two considerations give a normal force of 18 N as shown in Equation 1:

$$F_N = 15N/m \times 1.2m \quad (1)$$

In addition to that, a contact with of 2 mm between the rubber wiper and the PV surface is considered. Subsequently, a contact area can be calculated, and it's used to define cleaning pressure, as shown in Equation 2:

$$P = \frac{F_N}{A_c} \quad (2)$$

Considering the aforementioned information, a pressure of 0.0075 MPa is obtained. Therefore, the FEA simulation uses a pressure of 0.008 MPa that corresponds to the SC. In contrast, for the SDC, a pressure of 0.012 MPa -which is obtained by multiplying by a factor of 1.6 -is considered.

2.4.3. Frictional Drag

When the rubber wiper moves over the PV glass surface, a tangential force is applied into the cleaning arm. Subsequently, by considering a friction coefficient of $\mu = 1.0$, the frictional-drag force can be obtained by using Equation 3:

$$F_d = \mu \times F_N \quad (3)$$

In the SC conditions, the resulting drag force is 18 N, which is applied tangentially and opposite to the cleaning arm. Meanwhile, for the SDC conditions, the drag increased to 28.8 N as a consequence of multiplying by a factor value of 1.6.

Subsequently, the SC uses a gravity acceleration of 9810 mm/s², a pressure of 0.008 MPa, and a drag force of 18 N. In the SDC conditions, the gravity is 11770 mm/s², the pressure value is 0.012 MPa, and the drag force is 28.8 N.

2.5. Numerical Verification and Study Limitations

The presented PV cleaning device is evaluated via FEA analysis to obtain its static structural response. Consequently, the FEA analysis provided serves as a foundational study for a new generation of PV cleaning devices.

The selected simplified geometry, materials, applied boundary loads, and assumptions are part of the foundational analysis prior to the PV cleaning device fabrication. In this regard, the obtained stress concentration zone, contact pressures, and safety factors will serve as a description of the formulated scenarios, namely SC and SDC.

In both formulated scenarios, the same modelling assumptions are maintained, this will allow a equally comparation between the two states of operation of the proposed PV cleaning device. However, the absence of an experimental approach via the fabrication of the PV cleaning device is acknowledged as a limitation of the present study. In this regard, future studies will be dedicated to fabricating and testing the PV cleaning device, including strain gauge measurements, displacement readings, and contact pressure collection data. These future steps will allow a complete analysis of the device.

3. Results

3.1. Von Mises Stress Distribution

Based on the explained methodology, von Mises stressed that were obtained for the SDC and SC scenario a now presented. As depicted in Figure 4(a), the stress distribution for the SC case shows that the maximum von Mises stress was of 8.790 MPa.

It can be seen from the figure that the maximum stress is located in the region between the cleaning arm and the support component; this zone was identified as where the load transfer from the arm to the mobile carriage occurs. From the results, it can be seen that the obtained stress is below the yield strength of the corresponding material, which indicates that the device operates within the elastic range while its performing SC cleaning tasks.

Analogous, the resulting stress for the SDC scenario was reported in Figure 4(b). For this scenario, the maximum von Mises stress reached a value of 14.298 MPa. The obtained higher stress was expected as the SDC considers factored values of gravity, cleaning pressure, and drag force. Although the maximum stress was still below the yield strength value of the material, in this case ABS with 20 MPa and Aluminum 6061-T6 with 313 MPa.

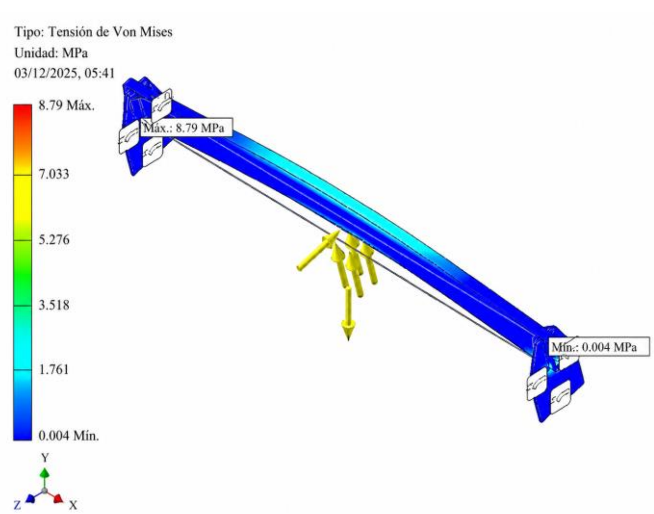

(a)

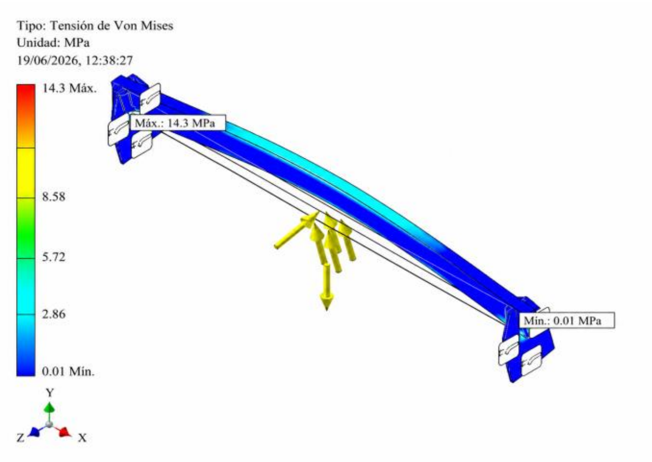

(b)

Fig. 4 Von Mises stress distribution obtained from FEA: (a) Service Case, (b) Strength Design Case

3.2. Displacement Analysis

The obtained displacement for the SC scenario is shown in Figure 5(a). It can be seen that the maximum obtained displacement was 0.145 mm and was located in the cleaning arm region, in which the applied pressure and tangential force are predominant. For this case, the observed deflection ratio of L/8277 indicated a rigid response under the applied loads.

Regarding the SDC scenario, the obtained displacement was 0.235 mm as shown in Figure 5(b), which is higher than the obtained displacement for the SC case. These values corresponded to a deflection ratio of L/5096. Despite the fact that the mechanical demand increased, the obtained displacements were still below the reference limit of L/250 (equivalent to 4.8 mm for a 1.2 m span). Consequently, the proposed arm was suitable for both the SC and SDC loading scenarios.

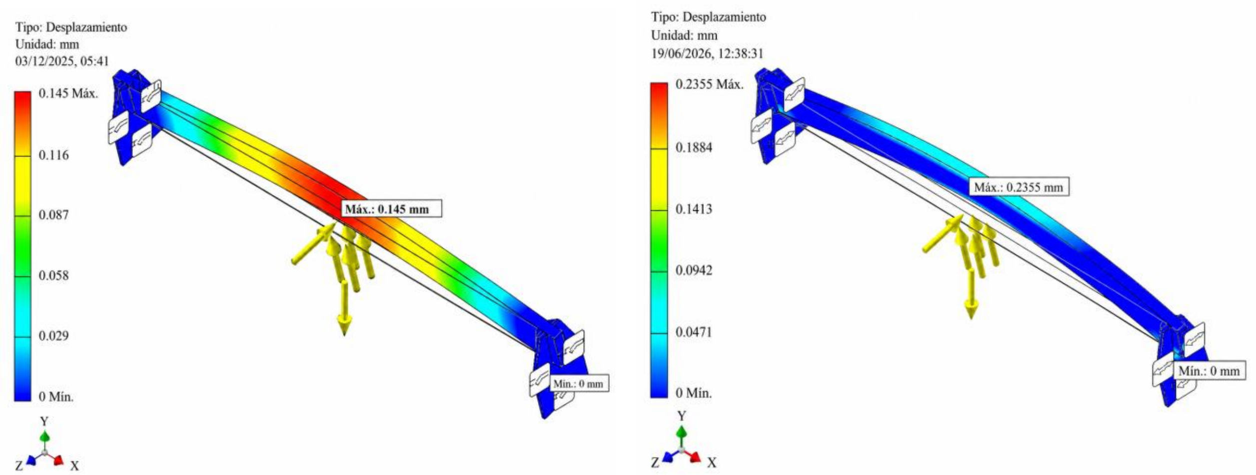

(a) **(b)**

Fig. 5 Total displacement diagrams obtained from FEA: (a) Service case, (b) Strength design case.

3.3. Safety Factor

The obtained safety factor was 15 for both the SC and SDC loading scenarios. This safety factor indicated that the proposed assembly was robust under the evaluated static conditions. Furthermore, the contact pressures were 8.938 MPa and 14.513 MPa for the SC and SDC, respectively. The observed increase was consistent with the factored pressure and friction load conditions used for the SDC scenario.

Similarly, the observed reaction forces of 220.451 N and 360.248 N for the SC and SDC, respectively, evidenced that the SDC value is higher than the SC value. Table 2 summarizes the obtained results of the FEA analysis for the SC and SDC scenarios. The table highlights that the SDC case evidence shows an approximate increase in the range of 62-63% over the SC scenario. However, both cases were considered suitable for the operation of the PV cleaning device.

Table 2. Comparison of finite element results between the Service Case and Strength Design Case

Parameter	SC	SDC	Variation (%)	Acceptance Criteria
Maximum von Mises stress (MPa)	8.79	14.298	+62.7	Below ABS yield strength of 20 MPa and Aluminum 6061-T6 yield strength of 313 MPa
Maximum displacement (mm)	0.145	0.235	+62.4	Below L/250 = 4.8 mm
Deflection ratio	L/8277	L/5096	-	Higher stiffness than the adopted serviceability reference

Maximum contact pressure (MPa)	8.938	14.513	+62.4	Consistent with the increase in factored loading
Reaction force (N)	220.451	360.248	+63.4	Consistent with the increase in applied loads
Safety factor	15	15	-	Did not fall below the software display threshold

4. Discussion

The results obtained from the PV cleaning device showed a suitable structural response under the two evaluated scenarios. In the SC scenario, the maximum obtained von Mises stress was 8.790 MPa, and the maximum reported displacement was 0.145 mm. On the other hand, the SDC scenario reported a maximum von Mises stress of 14.298 MPa and a maximum displacement of 0.235 mm. In the carried-out analysis, the factored load condition, which corresponds to the SDC scenario, evidenced an increase in the static response of approximately 62-63%; in both cases, the maximum reported stress was below the yield strength of the assigned material.

The proposed PV cleaning devices used a guided single axis for motion, lateral rails, and a mobile carriage that allowed the devices to move over the PV glass. In the proposed design, the applied load was predominant in the lateral supports of the device. The cleaning arm demonstrated stiffness in vertical displacements. In summary, the proposed device was evaluated prior to its prototyping.

When compared to drone-based cleaning devices, the presented device does not have flight time, battery, or outdoor stability limitations [13]. Furthermore, with respect to rotary or devices that are waterless, the presented device was less-far complex as it used linear guided motion and also avoids vibrations that are common in rotary cleaning solutions [14]. Monorail or robotic cleaning systems are also subject to structural analysis prior to implementation; this is aligned with the presented approach, as we evaluated the structural response of the cleaning arm and support elements prior to fabrication [15, 16].]. It must be pointed out that a simulation-based evaluation is relevant as it indicates the structural behavior of the PV device; this behavior has been demonstrated to be relevant as it prevents long-term damage [16].

A comparative benchmarking was developed for the proposed PV devices, as shown in Table 3. The comparation was made against the reported design in literature and patent documents.

Table 3. Qualitative benchmarking with existing photovoltaic cleaning approaches

Cleaning approach	Main limitation	Relation with the proposed device
Manual cleaning [9, 12]	Requires labor, water, access, and safety control	The proposed system automates the cleaning movement
Drone-based cleaning [13]	Limited by flight time, payload, battery, and wind stability	The proposed system avoids flight-related limitations.
Waterless/rotary systems [14]	May include rotating parts, vibration, and mechanical complexity	The proposed system uses guided linear wiping
Monorail/robotic systems [15, 16]	Robot-panel interaction and structural load must be controlled	The proposed system evaluates structural response through FEA
Patented guided cleaning systems [18, 19]	Structural verification is not always detailed	This study provides a preliminary FEA-based assessment

In practical engineering applications, the PV cleaning device can be installed on existing PV systems that are located on building rooftops, industrial facilities, and public structures. The presented design and its two lateral rails are suitable for integration into existing PV supporting frames. In addition, the presented cleaning arm guided from its sides was designed to reduce the mechanical demand on the PV glass and redirect the load to the lateral supports.

The scalability of the device is favorable as it can be replicated or adapted into multiple installations that contain PV modules in a row. However, a large-scale installation will require an additional analysis of rail alignment, and synchronization between all the motors, electrical protection, and ease of maintenance, to name a few points. The presented PV device may be relatively easier to fabricate than complex robotic or drone solutions. Although no quantitative cost table was made, based on the reduced complexity of the presented device, the cost may be reduced, and it must be mentioned that the main focus of this work is the novel device and its structural assessment. In this regard, the main maintenance cost is associated with the rubber wipe, belt transmission, and mobile carriages. However, the water tube may encounter obstructions caused by mineral deposits or suspended particles. The performance of the PV device may change depending on the installed area conditions. For dusty or arid environments, the wear in moving elements will increase. In windy areas, the device must be evaluated under a combined applied load that considers the wind. Therefore, the practical use of the PV device in different areas will require testing and environmental validation.

The main limitation of the presented approach is that no experimental or prototype fabrication of the PV device was carried out. In this sense, the presented results should be interpreted as a structural assessment of the PV devices prior to its implementation. The FEA model allowed the identification of stress concentration zones and displacements under the SC and SFC scenarios. However, fatigue analysis, dynamic motion, water flowing, or cleaning efficiency were not considered. For this reason, the presented analysis only supports the feasibility of the device and further studies will require prototyping, testing and field validation.

The main uncertainties regarding the structural assessment are related to the geometry simplification or the bounded contact conditions that exclude screws, and the deformable rubber wiper. These assumptions were included in order to reduce the model complexity, but that allows an acceptable assessment of the structural response of the PV device. Future work may include a mesh sensitivity analysis, dynamic modeling, structure and wind interaction, experimental measurements, and contact pressure sensors.

5. Conclusion

This study presented the design and structural assessment of a PV cleaning device that can be implemented in existing PV installations. The design includes a belt-driven and mobile carriage made of aluminum 6061-T6. The structural assessment was carried out using a static FEA analysis that considered factored load scenarios and the LRFD criteria. The outcomes of the simulation evidenced a suitable structural response of the PV cleaning device. In the SC scenario, the maximum von Mises stress was 8.790 MPa with a maximum displacement of 0.145 mm. For the SDC scenario, the von Mises stress increased to a value of 14.298 MPa, and its corresponding displacement was 0.235 mm. All the obtained values were located below the yield material limits and displacement criteria. Although the obtained safety factor was 15, further studies would be required to identify critical joints and supporting critical regions in order to increase the durability of the PV devices under constant operation.

The presented PV cleaning devices addressed limitations of rotary brushes that can induce vibration or flight time autonomy of drones. However, as no prototyping was presented, further studies should include experimental verification and sensor data. The future expected outcomes are:

- The fabrication of the PV device and correlating the FEA results with the experimental data.
- A modal analysis to evaluate the natural frequency of the device and avoid a resonance with the PV supporting frame.
- The evaluation of wind load in the PV device operation extends to specific environment analysis, such as coastal, dusty, or high-wind zones.

The presented study highlighted the design and structural assessment of PV cleaning devices that can be applied to multiple structures, and it's aligned with the civil engineering paradigm of sustainability. However, a complete validation of the device before its long-term operation would require prototyping, testing and field testing.

References

[1] Suqi Wang et al., "Integrating Renewable Energy into Building Energy Systems: A Systematic Review of Strategies, Barriers, and Policy Interfaces," *Discover Sustainability*, vol. 6, no. 1, pp. 1-22, 2025. [CrossRef] [Google Scholar] [Publisher Link]

[2] Ali Akbar Firoozi, D.O. Oyejobi, and Ali Asghar Firoozi, "Innovations in Energy-Efficient Construction: Pioneering Sustainable Building Practices," *Cleaner Engineering and Technology*, vol. 26, pp. 1-23, 2025.[CrossRef] [Google Scholar] [Publisher Link]

[3] Mohammad Ghiasi, Vahed Ghiasi, and Pierluigi Siano, "Renewable Energy Integration into Industrial and Residential Buildings: A Study Across Urban, Rural, and Coastal Areas," *IET Renewable Power Generation*, vol. 19, no. 1, pp. 1-17, 2025. [CrossRef] [Google Scholar] [Publisher Link]

[4] Abdelrahman O. Ali et al., "Advancements in Photovoltaic Technology: A Comprehensive Review of Recent Advances and Future Prospects," *Energy Conversion and Management: X*, vol. 26, pp. 1-28, 2025. [CrossRef] [Google Scholar] [Publisher Link]

[5] Sascha Lindig et al., "Performance Analysis and Degradation of a Large Fleet of PV Systems," *IEEE Journal of Photovoltaics*, vol. 11, no. 5, pp. 1312-1318, 2021. [CrossRef] [Google Scholar] [Publisher Link]

[6] Abdellahi Moulaye Rchid et al., "Comparative Analysis of AI-Driven Machine Learning Models for Fault Detection and Maintenance Optimization in Photovoltaic Systems," *Solar Energy and Sustainable Development Journal*, vol. 14, no. 1, pp. 361-378, 2025. [CrossRef] [Google Scholar] [Publisher Link]

[7] Sergio Llanos, Renán Orellana-Lafuente, and Daniel Felipe Sempértegui-Tapia, "Analysis of the Applicability of Photovoltaic Panel Cleaning Methods for South America-Distributed Generation Systems," *Journal Research & Development*, vol. 24, no. 1, pp. 107-120, 2024. [CrossRef] [Google Scholar] [Publisher Link]

[8] Basit Ali et al., "Experimental Investigation of Bird Dropping and Soiling on PV Panel Power Output in a Humid and Dusty Environment," *Sukkur IBA Journal of Emerging Technologies*, vol. 7, no. 1, pp. 1-14, 2024. [CrossRef] [Google Scholar] [Publisher Link]

[9] Nouhaila Najmi, and Ahmed Rachid, "A Review on Solar Panel Cleaning Systems and Techniques," *Energies*, vol. 16, no. 24, pp. 1-18, 2023. [CrossRef] [Google Scholar] [Publisher Link]

[10] Khaled M. Alawasa et al., "Comprehensive Assessment of Dust Accumulation Patterns and their Effects on Photovoltaic Plants in Semi-Arid Environments," *Cleaner Engineering and Technology*, vol. 29, pp. 1-13, 2025. [CrossRef] [Google Scholar] [Publisher Link]

[11] Haneen Abuzaid, Mahmoud Awad, and Mahmoud Awad, "Impact of Dust Accumulation on Photovoltaic Panels: A Review Paper," *International Journal of Sustainable Engineering*, vol. 15, no. 1, pp. 264-285, 2022. [CrossRef] [Google Scholar] [Publisher Link]

[12] M. Gandomzadeh et al., "Dust Mitigation Methods and Multi-Criteria Decision-Making Cleaning Strategies for Photovoltaic Systems: Advances, Challenges, and Future Directions," *Energy Strategy Reviews*, vol. 57, pp. 1-26, 2025. [CrossRef] [Google Scholar] [Publisher Link]

[13] S. Rehman et al., "Cleaning of Photovoltaic Panels Utilizing the Downward Thrust of a Drone," *Energies*, vol. 15, no. 21, pp. 1-14, 2022. [CrossRef] [Google Scholar] [Publisher Link]

[14] Charity M. Nkinyam et al., "Design and Implementation of a Waterless Solar Panel Cleaning System," *Unconventional Resources*, vol. 5, pp. 1-11, 2025. [CrossRef] [Google Scholar] [Publisher Link]

[15] Chengwei Shen et al., "Modeling and Analysis on Position and Gesture of End-Effector of Cleaning Robot Based on Monorail Bogie for Solar Panels," *9th International Conference, Intelligent Robotics and Applications*, Tokyo, Japan, pp. 122-133, 2016. [CrossRef] [Google Scholar] [Publisher Link]

[16] Murshiduzzaman et al., "Structural Prowess in Solar Panel Cleaning: A Comparative Study of Robotic Designs," *Journal of Applied Research and Technology*, vol. 22, no. 4, pp. 536-547, 2024. [CrossRef] [Google Scholar] [Publisher Link]

[17] Mustafa Eker, "Adaptive Drive Element for PV Panel Cleaning System: Linear BLDC Motor," *Electrical Engineering*, vol. 105, no. 1, pp. 407-417, 2023. [CrossRef] [Google Scholar] [Publisher Link]

[18] Chinmoy Prosun Saha, and Jeffrey Scott Pickles, "Photovoltaic Panel Cleaning System," *US Patent US11955927B2*, pp. 1-21, 2024. [Google Scholar] [Publisher Link]

[19] Tatsumi Tanaka, "Solar Panel Cleaning System," *European Patent EP3817222A1*, pp. 1-24, 2021. [Publisher Link]

[20] "ASM Material Data Sheet" [Online]. Available: https://asm.matweb.com/search/specificmaterial.asp?bassnum=ma6061t6

[21] ASCE 7-16 LRFD Load Combinations, SkyCiv, 2025. [Online]. Available: https://skyciv.com/docs/tech-notes/load-combinations/asce-7-10-lrfd/